# An *ab initio* study of the interaction of graphene and silicene with one-, two-, and three-layer planar silicon carbide

Alexander Y. Galashev [a,b,*], Alexey S. Vorob'ev [a]

[a] Institute of High Temperature Electrochemistry, Ural Branch, Russian Academy of Sciences, Academicheskaya Str., 20, Ekaterinburg, 620990, Russia
[b] Ural Federal University Named After the First President of Russia B.N. Yeltsin, Mira Str., 19, Ekaterinburg, 620002, Russia

## ARTICLE INFO

## ABSTRACT

Structural, energy and electronic properties of two-dimensional semiconductors are found to differ from those inherent in natural ones, due to $sp^2$ hybridization caused by a decrease in thickness down to the atomic scale. Hybrid 2D semiconductors can combine unique properties of each component, which makes them promising materials for application in electronics, energy storage devices, sensors and catalysts. The unique properties of such semiconductors appear not only due to the effect of size reduction or transition to the discharge of nanoscale objects, but also due to the modification of the electronic structure. In this work, on the basis of DFT calculations, we investigate the geometrical and electronic structures of two hybrid two-dimensional semiconductors created by combining graphene or silicene with silicon carbide, consisting of 1–3 layers. The geometric and energy characteristics of the systems are calculated, and the dependence of the structural parameters, as well as the band structure and density of electronic states, on the number of layers present in silicon carbide are determined. In the "graphene- SiC" system, in the presence of 1–3 layer silicon carbide, a very narrow band gap opens (0.015–0.022 eV). For the "silicene on one- and two-layer silicon carbide" system, a small band gap also appears (0.047 and 0.078 eV, respectively). In the presence of silicene and three layers of silicon carbide in the system, the direct band gap becomes the indirect one. Silicene, in contrast to graphene, shows a high sensitivity to the thickness of the adjacent silicon carbide.

## 1. Introduction

Recently, in the 2D materials research area, there has been a trend towards the implementation of hybrid materials and heterostructures formed by different semiconductors. The development of next-generation materials will combine the advantages of well-known semiconductors with the exclusive properties of 2D materials such as graphene or silicene. Graphene is a two-dimensional allotropic material with unique electronic and mechanical properties, that was experimentally obtained in 2004 [1,2]. An experimental study on the SiC electrodes for lithium-ion batteries (LIBs) was carried out in Ref. [3]. The integration of graphene and SiC is a promising approach creating a new advantageous hybrid material [4]. Graphene can be obtained by decomposition (sublimation) of SiC [5]. The SiC substrate can also be used in chemical vapor deposition (CVD) and molecular beam epitaxy (MBE) methods for producing graphene. Flexural lattice vibrational phonon modes provide the record-high thermal conductivity of graphene $\sim 5 \times 10^3$ W m$^{-1}$ K$^{-1}$ [6].

Free carriers in graphene behave like massless relativistic quasiparticles, the mobility of which is $\sim$100,000 cm$^2 \times$ V$^{-1}$. There is no band gap in the graphene band structure, and Dirac cones are formed at points K and K'. There are several forms of graphene, such as nanoribbons, nanosheets, nanoplates [7] and 3D-graphene [8]. Unique electronic properties of graphene stem from the $sp^2$ hybridization of the electron orbitals of carbon atoms, resulting in the carbon atom forming three planar bonds. The experimental production of graphene gave impetus to the search for new two-dimensional (2D) materials, which represent a new class of promising materials for a wide range of applications. The family of 2D substances has been expanded with such new materials as hexagonal boron nitride [9], borophene [10], germanene [11], phosphorene [12], and silicene [13].

Silicene, a two-dimensional analog of the graphene, that was first experimentally obtained on an Ag (111) substrate with the formation of the 4 × 4 supercell [13]. Subsequently, single-layer silicene was

* Corresponding author. Institute of High Temperature Electrochemistry, Ural Branch, Russian Academy of Sciences, Academicheskaya Str., 20, Ekaterinburg, 620990, Russia.
*E-mail address:* alexander-galashev@yandex.ru (A.Y. Galashev).

epitaxially synthesized on Ir (111) [14], MoS$_2$ [15], ZrB$_2$ (0001) [16], ZrC (111) [17], graphite [18] and Ru (0001) [19] substrates. Theoretically, using modeling by the methods of classical molecular dynamics and quantum mechanics, the interactions of silicene with copper [20], nickel [21], silver [22,23], aluminum [24,25] and graphite [26–28] substrates were studied. Recently, a breakthrough has been made in the synthesis of autonomous silicene by chemical exfoliation using CaSi$_2$ as a precursor [29]. Autonomous ideal silicene is a narrow-gap semiconductor with a band gap of 27 meV [30]. Due to its unique electronic and structural properties, silicene can be used in many applications, including field-effect transistors [31], gas sensors [32], and thermoelectric devices [33].

Bulk SiC exists in more than 200 crystalline forms [34], some of them have a three-dimensional hexagonal crystal structure. The energy of the C face of layered SiC is 2.46 times lower than the corresponding value for the Si face. Therefore, graphene of high structural quality can be grown over large areas of the Si face of SiC. In the case of obtaining two-layer graphene on the Si-face, the first carbon layer is covalently bonded to the SiC substrate and is metallic, while the second C layer turns out to be semimetallic and has Dirac cones in the electronic spectrum [35].

In [36–38], a planar structure of silicon carbide was predicted, which is identical to graphene, but with a bond distance of 1.77–1.79 Å and a band gap of 2.5–2.6 eV. It was possible to experimentally synthesize flakes of quasi-planar silicon carbide via high-temperature thermochemical substitution reactions of exfoliated graphene with silicon powder in Refs. [39,40]. An experimental study of the behavior of nanosized SiC grains accumulating in the pores of graphene oxide (GO), as well as *ab initio* modeling of single-layer planar silicon carbide, was performed in Ref. [41].

One-dimensional silicon carbide (1D structure of SiC) was also synthesized in the form of silicon-carbon tubes, which have high thermal stability and unique electronic properties [42]. Such tubes can be used to store hydrogen, while sulfur doping leads to an increase in the hydrogen capacity of a silicon carbide tube [43].

Graphene and its derivatives are highly chemically inert and hydrophobic, for example, a polymer composite of graphene oxide on copper [44] forms a crack-free highly dense coating with a uniform thickness. This coating is highly resistant to oxidation and corrosion in a chloride environment.

Young's modulus shows that the in-plane stiffness of graphene is more than 6 times higher than that of silicene [45]. The graphene/SiC system can be used as a platform for the synthesis of new forms of 2D materials, such as 2D GaN [46], 2D InN [47], and 2D AlN [48] by controlling intercalation of precursors at the graphene/SiC interface. The preparation and application of van der Waals (vdW) heterostructures constructed from various 2D materials are described in Refs. [49–51]. On the basis of these developments, it is proposed to create tunneling field-effect transistors (TFETs) [52], an interband tunneling transistor [53] and a transistor based on field-effect modulation of the Schottky barrier (barristor) [54].

In this work, the interaction between single-layer silicene or graphene and one-, two-, and three-layer planar silicon carbide is studied using methods based on the density functional theory, a special attention is drawn to the changes in the structural, energy, and electronic properties of these 2D nanomaterials.

## 2. Model

The results presented in this paper are based on DFT calculations in a generalized gradient approximation (GGA). To carry out calculations using SIESTA codes [55], a hybrid cluster-type computer "URAN" (N.N. Krasovskii Institute of Mathematics and Mechanics UB RAS) with a peak performance of 216 Tflop/s and 1864 CPU was used. The parameters characterizing the stability and structure of the investigated hybrid 2D materials, represented by silicene and graphene, placed on one-, two-,

and three-layer planar silicon carbide (2D-SiC), were calculated using the following model. Graphene, silicene, and 2D silicon carbide were modeled as superlattices: 5 × 5 (50 carbon atoms), 3 × 3 (18 silicon atoms), and 4 × 4 (16 carbon atoms and 16 silicon atoms), respectively. The minimum scaling was required to align the superlattices of graphene and two-dimensional silicon carbide, since the lengths of the translation vectors of these lattices differed by less than 1%. More significant scaling was performed to align silicene and 2D-SiC superlattices due to the greater difference in the sizes of these cells. In this case, both supercells were scaled, i.e., the silicene lattice increased by 1.8% and the two-dimensional silicon carbide superlattice decreased by 1.8%. Fig. 1 shows a view of aligned superlattices. The initial distances between the layers of silicon carbide, silicon carbide and graphene, as well as 2D-SiC and silicene were 2.32, 3.52, and 3.1 Å, respectively. In the first two cases, these characteristics were identical to the corresponding distances obtained in Ref. [38]. The distance between silicene and planar silicon carbide was determined as the average value between the distance from silicene to the graphite substrate (3.44 Å) [28] and the distance between two layers of silicene (2.75 Å) [56]. Layers of two-dimensional silicon carbide were formed in accordance with the AA′ configuration (the silicon atom is located above the carbon atom and vice versa), which, according to Ref. [38], is the most stable configuration for 2D-SiC. In each of the considered cases, the translation period in the z-direction was 35 Å. The geometric optimization using the DRSLL approximation [57,58], which takes into account van der Waals interactions, was carried out for all considered systems. The dynamic relaxation of atoms continued until the total energy was converged to less than 0.0001 eV atom-1. The cutoff energy of the plane wave basis set was 400 Ry. The setting of the Brillouin zone and ensuring the convergence of the GGA results was carried out using a k-grid-Monkhorst-Pack mesh [59] of 10 × 10 × 1.

For the systems under study, the following characteristics were calculated:

1. The adhesion energy between silicene/graphene and two-dimensional silicon carbide was determined according to the expression:

$$E_{\text{adh}} = \frac{E_{tot} - E_{\text{C/Si}} - E_{\text{SiC}}}{N_{\text{el}}}, \tag{1}$$

where $E_{\text{tot}}$ is the total energy of the entire system, $E_{\text{C/Si}}$ is the total energy, calculated for graphene or silicene, $E_{\text{SiC}}$ is the total energy, calculated for silicon carbide, and $N_{\text{el}}$ is the number of unit cells of graphene (25) or silicene (9) in the system.

2. The energy of adhesion between layers of silicon carbide was determined according to the expression:

$$E_{\text{coh}}^{\text{SiC}} = \frac{E_{\text{SiC}} - \sum_l E_{\text{lSiC}}}{N}, \tag{2}$$

where $E_{\text{lSiC}}$ is the total energy calculated for the silicon carbide layer, and $N$ is the number of atoms in system.

3. The bond energy in "graphene - silicon carbide (C–SiC)" or "silicene-silicon carbide (Si–SiC)" was determined as:

$$E_{\text{b}} = \frac{E_{\text{Tot}} - N_{\text{Si}}E_{\text{Si}} - N_{\text{C}}E_{\text{C}}}{N_{\text{Si}} + N_{\text{C}}}, \tag{4}$$
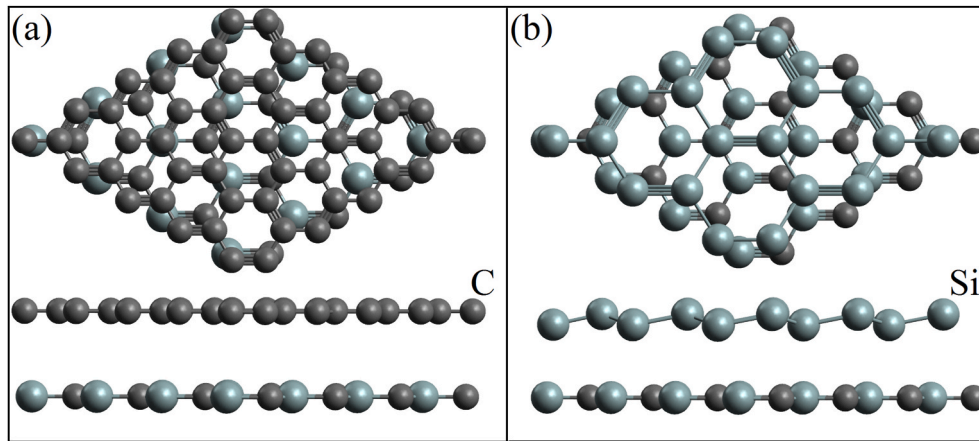
**Fig. 1.** Geometrical structure of superlattices of (a) graphene 5 × 5 and silicon carbide 4 × 4, (b) silicene 3 × 3 and silicon carbide 4 × 4.

where $E_{\text{Si/C}}$ is the total energy calculated for one Si or C atom, and $N_{\text{Si}}$ and $N_{\text{C}}$ denote the number of silicon and carbon atoms in the system.

4. The bond energy in a sheet of silicene, graphene, or silicon carbide was determined as:

$$E_{\text{b}}^{\text{Si/C/SiC}} = \frac{E_{\text{Si/C/SiC}} - N_{\text{Si}} E_{\text{Si}} - N_{\text{C}} E_{\text{C}}}{N_{\text{Si}} + N_{\text{C}}}, \qquad (5)$$

where $E_{\text{Si/C/SiC}}$ is the energy calculated for silicene, graphene, or silicon carbide.

5. The expression for calculating average displacements relative to ideal free-standing configurations of silicene, graphene, and silicon carbide is as follows:

$$\Delta k(\text{Si/C/SiC}) = \frac{\sum_n abs((k_1 - k_0) - \overline{k})}{N}, \qquad (6)$$

where $k_1$ is the $x, y$ or $z$ coordinate after geometric optimization, $k_0$ is the $x, y,$ or $z$ coordinate before geometric optimization, $\overline{k}$ is the average value obtained for the $k_1 - k_0$ coordinate difference over all particles, introduced to exclude the parallel displacement of the system, and $N$ is the number of particles in the system.

We also determined the potential energy barrier for electrons formed at the metal-semiconductor junction (a Schottky barrier). A Schottky barrier (SB) was calculated as the energy difference from the Fermi level to the conduction band minimum of silicon carbide.

To calculate atomic charges, we used the Voronoi strain density (VDD) method. This method was implemented in calculating the value of the electron density without the explicit usage of basis functions. The method assumes that electron density flows to or from a specific atom due to the bond formation. The overflow density is calculated by spatial integration of the deformation density over the Voronoi atomic cell. This method was chosen due to its advantage over the well-known methods of Mulliken and Bader [60]. As a rule, the magnitude of the Mulliken charges strongly depends on the choice of the basis set. The Bader charges are often unrealistic because their calculation is associated with an overestimation of the ionic nature of bonds, even in the case of co-valent bonds. The Hirshfeld and VDD charges, in most cases, have close realistic and chemically relevant values. The advantage of the VDD method is the transparency of the approach due to the simple geometric division of space.

## 3. Results and discussion

Information on the structural and adhesive characteristics of hybrid materials is important for determining the possibility and prospects of their use. Table 1 shows the following calculated geometrical and energy characteristics of the system: the bond energy in the compound ($E_{\text{b}}$); the bond energy in graphene or silicene ($E^{\text{C/Si}}_{\text{b}}$); the bond energy in silicon carbide ($E^{\text{SiC}}_{\text{b}}$); the adhesion energy between graphene/silicene and silicon carbide ($E_{\text{adh}}$); the cohesion energy between silicon carbide layers ($E^{\text{SiC}}_{\text{coh}}$); the width of the band gap (BG); the Schottky barrier (SB); displacements in the $x, y,$ and $z$ directions relative to an ideal freestanding two-dimensional silicon carbide and silicene/graphene ($\Delta x$ (SiC), $\Delta y$ (SiC), $\Delta z$ (SiC), $\Delta x$ (Si/C), $\Delta y$ (Si/C), and $\Delta z$ (Si/C)); the distance between graphene/silicene and silicon carbide along the $z$ axis ($\Delta Z$ (C/Si–SiC)); the distance between the silicon carbide layers along the $z$ axis ($\Delta Z$ (SiC)); the distance between the silicene sublattices along the $z$ axis ($\Delta z$ (Si–Si)); the lengths of the Si–C bond in silicon carbide (Si–C); bond lengths in graphene/silicene (C–C/Si–Si); total charges of silicon ($Q_{\text{V}}$(SiC–Si)) and carbon ($Q_{\text{V}}$(SiC–C)) in SiC, as well as silicene or graphene ($Q_{\text{V}}$(Si/C)), calculated by the Voronoi method proposed in Ref. [60].

The bond energy in the "graphene - silicon carbide (C–SiC)" compound ($E_{\text{b}}$) does not depend on the number of SiC layers, while in the "silicene-silicon carbide (Si–SiC)" compound it increases from 5.723 to 6.253 eV. An increase in the bond energy in the "silicene-silicon carbide" nanocomposite accompanied with an increase in the number of 2D-SiC layers is explained by two reasons. First, the adhesion energy $E_{\text{adh}}$ increases at ~6.46 times, i.e. stronger bonds are formed between silicene and the top layer of silicon carbide. Second, there is an enhancement in the interaction between the SiC layers. For example, as the number of SiC layers increases from two to three, the cohesion energy between the SiC layers increases by ~97%. However, there is a weakening in the interaction between silicon atoms in the silicene sheet (the $E^{\text{Si}}_{\text{b}}$ energy decreases by ~ 3.8%). This may be due to an increase in the interaction between silicene and 2D-SiC. The bond energy between silicon atoms in a silicene sheet located on a planar silicon carbide sheet is 5.5% lower than the Si–Si bond energy in a freestanding ideal silicene sheet [61]. The discrepancies are associated with the interaction between silicene and silicon carbide as well as an increase in the translation vectors of the silicene supercell by 1.8%. The bond energy between carbon atoms in a graphene sheet obtained in the present study is ~6.9% higher than the value $E^{\text{C}}_{\text{b}}$ for a 4 × 4 graphene supercell in Ref. [62]. This can be explained by three reasons. First, the interaction between the graphene sheet and two-dimensional silicon carbide occurs. Second, a 5 × 5 supercell was used in our work. Third, we used a different approximation (DRSLL instead of B3LYP) which takes into account van der Waals interactions.

**Table 1**
Geometrical and energy characteristics of the studied systems*.

| Properties | C | | | Si | | |
|---|---|---|---|---|---|---|
| $N_{SiC}$ | 1 | 2 | 3 | 1 | 2 | 3 |
| $E_b$, eV | 7.289 | 7.194 | 7.286 | 5.723 | 6.090 | 6.253 |
| $E^{C/Si}_b$, eV | 8.584 | 8.584 | 8.583 | 4.323 | 4.216 | 4.160 |
| $E^{SiC}_b$, eV | 6.461 | 6.511 | 6.579 | 6.433 | 6.455 | 6.480 |
| $E_{adh}$, eV | 0.111 | 0.120 | 0.120 | 0.274 | 1.148 | 1.771 |
| $E^{SiC}_{coh}$, eV | – | 0.050 | 0.326 | – | 0.207 | 0.407 |
| BG, eV | 0.015 (direct) | 0.019 (direct) | 0.022 (direct) | 0.047 (direct) | 0.078 (direct) | 0.017 (indirect) |
| SB, eV | 0.0081 | 0.0097 | 0.0183 | 0.0190 | 0.0192 | 0.0032 |
| $\Delta x$ (SiC), Å | 0.013 | 0.009 | 0.027 | 0.003 | 0.031 | 0.034 |
|  |  | 0.009 | 0.030 |  | 0.027 | 0.013 |
|  |  |  | 0.028 |  |  | 0.015 |
| $\Delta y$ (SiC), Å | 0.010 | 0.011 | 0.025 | 0.003 | 0.027 | 0.024 |
|  |  | 0.012 | 0.029 |  | 0.032 | 0.023 |
|  |  |  | 0.030 |  |  | 0.025 |
| $\Delta z$ (SiC), Å | 0.005 | 0.017 | 0.182 | 0.130 | 0.221 | 0.290 |
|  |  | 0.005 | 0.186 |  | 0.340 | 0.302 |
|  |  |  | 0.251 |  |  | 0.249 |
| $\Delta x$ (Si/C), Å | 0.012 | 0.011 | 0.013 | 0.054 | 0.065 | 0.097 |
| $\Delta y$ (Si/C), Å | 0.012 | 0.012 | 0.013 | 0.003 | 0.043 | 0.066 |
| $\Delta z$ (Si/C), Å | 0.028 | 0.047 | 0.061 | 0.041 | 0.389 | 0.301 |
| $\Delta Z$ (C/Si–SiC), Å | 3.663 | 3.604 | 3.654 | 3.677 | 2.728 | 2.596 |
| $\Delta Z$ (SiC), Å | – | 3.553 | 2.701 | – | 3.005 | 2.612 |
|  |  |  | 2.642 |  |  | 2.651 |
| $\Delta z$ (Si–Si), Å | – | – | – | 0.487 | 0.875 | 0.868 |
| Si–C, Å | 1.783 | 1.784 | 1.875 | 1.782 | 1.847 | 1.915 |
| C–C/Si–Si, Å | 1.427 | 1.427 | 1.427 | 2.398 | 2.436 | 2.475 |
| $Q_V$(SiC–Si) | 7.182 | 14.596 | 21.299 | 7.422 | 13.809 | 19.857 |
| $Q_V$(SiC–C) | −7.498 | −14.950 | −21.640 | −7.442 | −14.061 | −20.305 |
| $Q_V$(Si/C) | 0.316 | 0.354 | 0.341 | 0.020 | 0.252 | 0.448 |

* $N_{SiC}$ is the number of SiC layers; $E_b$ is the bond energy in the compound, $E^{C/Si}_b$ is the bond energy in graphene or silicene; $E^{SiC}_b$ is the bond energy in silicon carbide; $E_{adh}$ is the adhesion energy between graphene/silicene and silicon carbide; $E^{SiC}_{coh}$ is the cohesion energy between silicon carbide layers; BG is the width of the band gap; SB is the Schottky barrier; $\Delta x$(SiC), $\Delta y$(SiC), $\Delta z$(SiC), $\Delta x$(Si/C), $\Delta y$(Si/C), and $\Delta z$(Si/C) are displacements in the $x$, $y$, and $z$ directions relative to an ideal free-standing two-dimensional silicon carbide and silicene/graphene; $\Delta Z$(C/Si–SiC) is the distance between graphene/silicene and silicon carbide along the $z$ axis; $\Delta Z$ (SiC) is the distance between the silicon carbide layers along the z axis; $\Delta z$(Si–Si) is the distance between the silicene sublattices along the $z$ axis; Si–C are the lengths of the Si–C bond in silicon carbide; C–C/Si–Si denotes bond lengths in graphene/silicene $Q_V$(SiC–Si) and $Q_V$(SiC–C) denote the Voronoi charges calculated for the silicene and carbon in SiC, respectively; $Q_V$(Si/C) denotes the Voronoi charges calculated for the silicene or graphene sheet.

Materials such as graphene and silicene are extremely thin and have a high specific surface area. As a result, they can be easily deformed by surface forces when approaching an adjacent surface to distances in the nanometer range. The adhesion interaction is critical when using layered hybrid materials in micro- and nanoelectromechanical systems [63], flexible devices [64], and surface coatings [65]. Adhesion is also important in the production of graphene and silicene by chemical vapor deposition (CVD). It can be seen from Table 1 that the adhesion energy of silicene to single-layer SiC is almost 2.5 times higher than the analogous characteristic for graphene. In the case of three-layer SiC, the difference in adhesion energies for silicene and graphene increases and reaches 14.7 times. The adhesion energy of graphene to SiC does not increase, and the gap between the graphene sheet and the top silicon carbide layer widened by 1.4% when the third layer is added to the two-layer SiC. During a similar operation in the "silicene-(2D-SiC)" system the silicene sheet is closer to SiC by almost 4.8% and the adhesion energy increases by 54%. The addition of the next (third) SiC layer to the "silicene-(2D-SiC)" system initiates a transition to the bulk structure of silicon carbide. As a result, silicene in close contact with SiC layer also changes its structure, binding even more strongly to SiC. Graphene, in contrast to silicene, turned out to be much less sensitive to the structural rearrangement occurring in silicon carbide. In all the cases considered, graphene is much weaker bound to 2D-SiC than silicene. The calculated value of the adhesion energy between graphene and two- (three-) layer silicon carbide (0.120 eV) is in good agreement with the experimentally determined value of the adhesion energy between graphene and the silicon substrate (0.129 eV) [66], but that is inferior to the adhesion energy between graphene and SiO₂ substrate (0.163 eV) [67].

An increase in the cohesion and adhesion energies between the layers of silicon carbide, silicene and silicon carbide is accompanied by geometrical rearrangements. Fig. 2 shows the geometrical structures of graphene and silicene on one-, two-, and three-layer silicon carbide. The calculated average relative displacements in the sheets of silicene and silicon carbide along the $x$ and $y$ axes indicate small (not exceeding 0.1 Å) atomic displacements for all considered silicene - silicon carbide nanocomposites, which indicates that the hexagonal structure of these materials is preserved. However, the average displacements along the $z$ axis with an increase in the number of silicon carbide layers exceed 0.1 Å, which is associated with strong geometric rearrangements in the systems. In other words, these rearrangements are mainly reflected in the interlayer distances (i.e. in the z direction). Thus, as the number of 2D-SiC layers increases, the distances between silicene and silicon carbide, as well as between silicon carbide layers, decrease from 3.677 to 2.596 Å and from 3.005 to ~2.632 Å, respectively. As a result, the lengths of Si–C bonds in silicon carbide sheets increase by ~7.4%. The interaction of silicene with two- and three-layer silicon carbide leads to an increase in the distance between the silicene sublattices from 0.487 to 0.868 Å, resulting in an increase in the lengths of Si–Si bonds in the silicene sheet by ~3.2%.

The average relative displacements of C atoms in graphene interacting with one-, two-, and three-layer silicon carbide do not exceed 0.1 Å, which indicates the preservation of the flat cellular structure of the graphene sheet. While two-dimensional silicon carbide interacting with graphene retains its two-dimensional structure when the number of layers is less than 3. However, an increase in the number of layers up to 3 causes geometric rearrangements. This is how the Si–C bond lengths increase by ~5.1%, mainly due to geometric rearrangements along the z axis. The obtained energy characteristics reflect the geometric rearrangements occurring in the system. So as the number of 2D-SiC layers increases from 2 to 3, the cohesion energy between the SiC layers
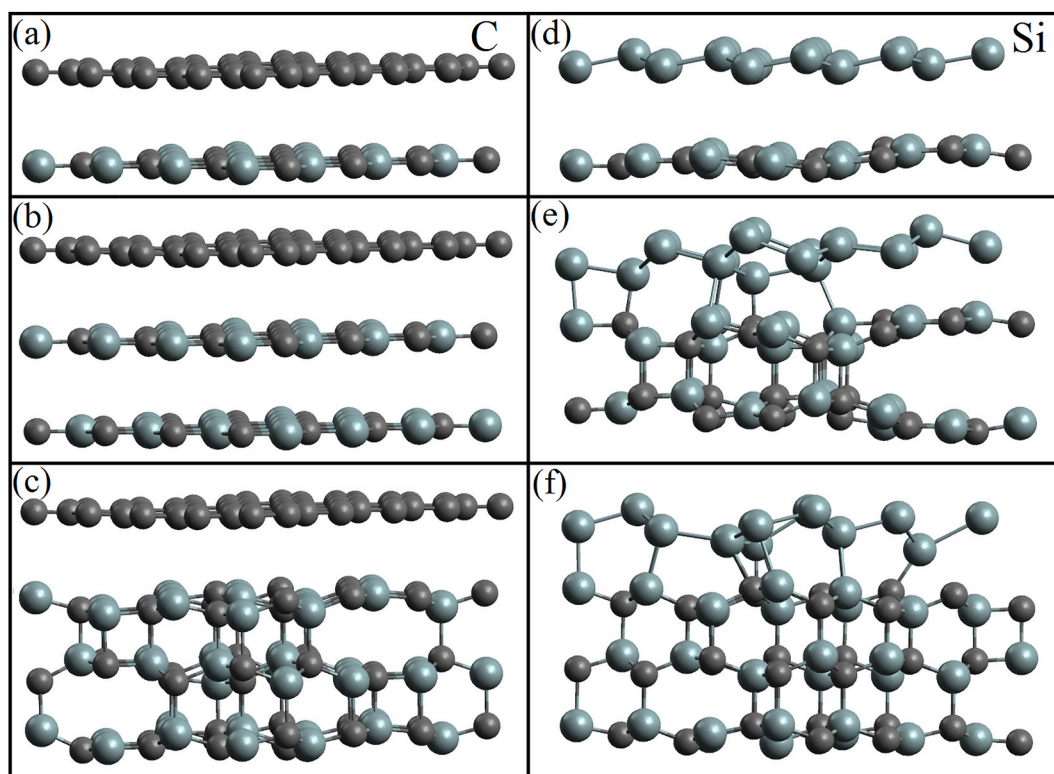
**Fig. 2.** Geometrical structure of systems after geometric optimization, where a, b and c illustrate graphene, and d, e and f illustrate silicene on one-, two- and three-layer silicon carbide, respectively.

increases from 0.05 to 0.326 eV.

Silicon atoms in SiC have a positive charge (~0.44 a.u.), while carbon atoms are negative (~−0.45 a.u.). The total charge of all atoms in silicon carbide in all considered cases is negative. At the same time, the charge of graphene or silicene sheets is positive. That is, the systems studied here contain a p-n junction. Moreover, silicene and graphene are p-type semiconductors, and silicon carbide is n-type. We calculated the Schottky barriers to indicate the appearance of a potential difference between graphene (silicene) and one-, two-, and three-layer silicon carbide. The barrier obtained for graphene on 2D-SiC (0.008–0.018 eV) is smaller than the barrier obtained in Ref. [68] (0.85 eV) and [69] (0.36 eV) for graphene based on the bulk 4H–SiC phase that consists of an equal number of cubic and hexagonal bonds with ABCB stacking sequences. The values of the Schottky barriers obtained in the present research turn out to be extremely low due to the presence of a very close contact between the quasi semiconductor and the quasi metal, due to the smallness of their sizes. Such an ideal contact and purity of touching materials cannot be obtained experimentally. The study of the contact between the forest of carbon nanotubes (CNT) and silicon carbide showed that the height of the Schottky barrier of the CNT/SiC contact was in the range of 0.40–0.45 eV [70]. Graphene/silicene-SiC hybrid systems with a very low Schottky barrier (<0.1 eV) can be recommended for use in a n-channel metal-oxide-semiconductor field-effect-transistor (MOSFET) with a Schottky barrier. Devices of this type require lower Schottky barriers to obtain a higher excitation current. Note that a low Schottky barrier (<0.1 eV) was experimentally determined in the PtEr silicide system on a n-type silicon substrate [71].

Fig. 2c and f shows the geometrical structures of graphene and silicene on three-layer silicon carbide, respectively. It is seen that geometric rearrangements in silicon carbide change its planar structure to the structure of the corresponding bulk phase. However, due to the limitations imposed by the supercell and the insufficient number of SiC layers, some transition phases similar to the 4H–SiC phase are observed [68]. The Si–C bond lengths in the hybrid nanocomposites shown in Fig. 2c

and f, are equal to 1.875 and 1.915 Å. These values are close to the corresponding bond length of 1.89 Å [68] in bulk 4H–SiC. Fig. 3 shows the structure of 4H–SiC and parts of the structures obtained by us, which are similar to 4H–SiC.

Fig. 4 shows the geometrical structures of one- (a), two-layer (c), and three-layer (e) 2D-SiC obtained in the presence of a graphene sheet, as well as the corresponding band structures (b), (d), (f) in these systems. The graphene sheet is neither shown in Fig. 4 (a), (c), (e) nor its direct contribution is shown in Figures (b), (d), (f). As the number of silicon
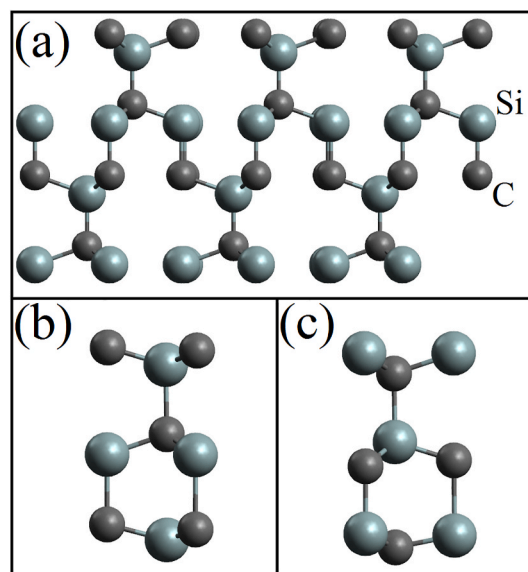


**Fig. 3.** Geometrical structure of (a) ideal 4H–SiC and some parts obtained during the interaction of three-layer planar silicon carbide with (b) graphene and (c) silicene.
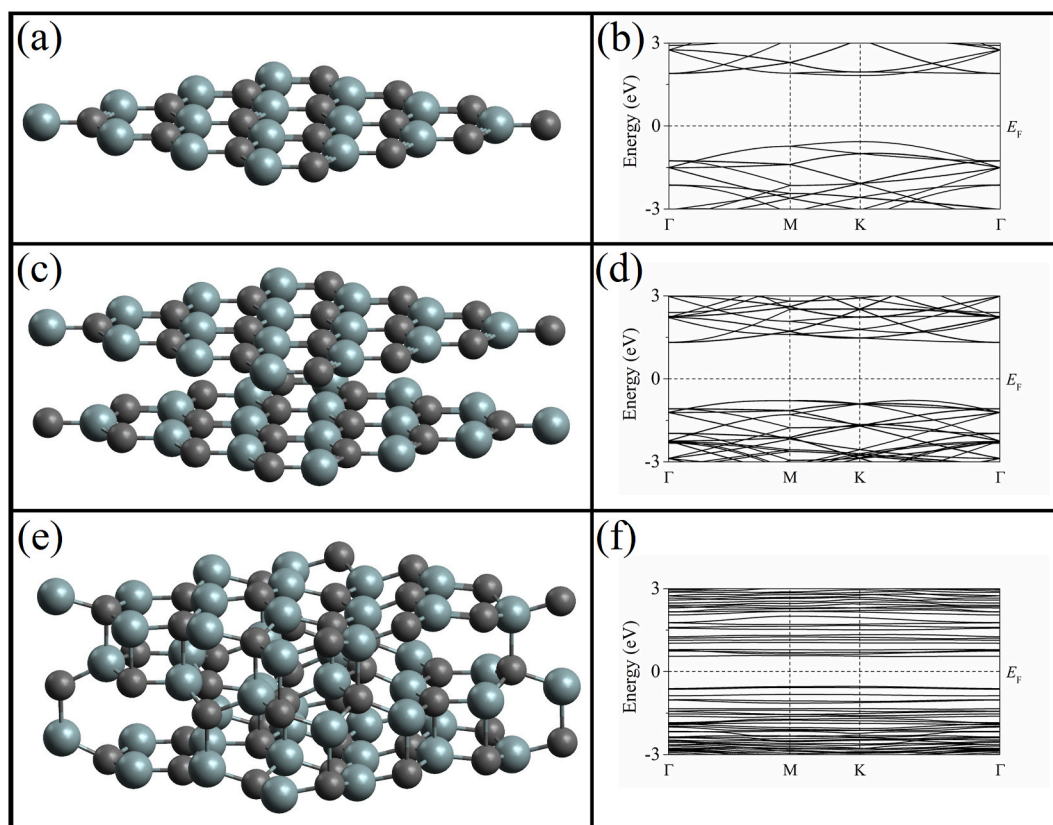
**Fig. 4.** Geometrical structures of (a) one-, (c) two- and (e) three-layer 2D-SiC obtained together with the attached graphene sheet, as well as the corresponding band structures (b), (d), (f) in this system without a direct contribution from the graphene sheet.

carbide layers increases, the band gap changes. Therefore, a system with a single-layer silicon carbide has a bandgap of 2.391 eV, the addition of a second layer reduces the band gap to 2.099 eV, and in a system with three-layer 2D-SiC, the band gap is 1.08 eV.

Fig. 5 shows the geometrical structures of (a) one-, (c) two-, and (e) three-layer 2D-SiC obtained in the presence of a silicene sheet, which is not illustrated. Fig. 5 (b), (d), (f) also show the band structures in these systems, excluding direct contributions from silicene sheet. As in the systems, including a graphene sheet, in the presence of a silicene sheet, the band gap narrows as the number of layers of two-dimensional silicon carbide increases. For example, systems with single-layer and two-layer silicon carbide have band gaps of 2.464 and 0.672 eV, respectively. When the number of silicon carbide layers reaches three, the resulting hybrid system acquires conductive properties.

Fig. 6 reflects the geometrical structures of graphene (Fig. 6 a) and silicene (Fig. 6 c) placed on 4H–SiC. This figure also shows the band structures of the systems: (b) "graphene on 4H–SiC" and (d) "silicene on 4H–SiC". To align 4H–SiC and a $3 \times 3$ silicene supercell as well as a $5 \times 5$ graphene supercell, the bond lengths in the $x$ and $y$ directions in 4H–SiC were reduced by 2%. All silicon and carbon atoms included in the bulk 4H–SiC phase were fixed, i.e. did not undergo dynamic relaxation. While the relaxation of atoms included in silicene and graphene was available in all possible directions. Fixing the positions of the C and Si atoms makes it possible to preserve the structure of the bulk 4H–SiC phase in the presence of a small number of silicon carbide layers. It can be seen that, after passing through relaxation in graphene (silicene), hexagonal silicon and carbon rings are retained. The opening of the band gap in systems containing graphene and silicene sheets was not achieved due to a very small number of SiC layers, which represent the bulk 4H–SiC phase. It can be seen that in the band structure of graphene placed near two bilayers of the 4H–SiC structure, the Dirac cone, which is located below the Fermi level (Fig. 6b), is retained. However, in the band

structure of silicene, similar to that presented above, the Dirac cone is not preserved due to its strong interaction with silicon carbide.

Figs. 7 and 8 show the band structures and spectra of electronic states (DOS) of graphene and silicene located on silicon carbide with different number of layers in 2D-SiC, respectively. All systems obtained are narrow-gap semiconductors. It can be seen that in graphene on silicon carbide, for all the number of 2D-SiC layers considered, there is the band gap of 15–22 meV, while the Dirac cones are preserved. The band gap in free-standing silicene is 27 meV. This characteristic in the interaction between silicene and single-layer and two-layer planar silicon carbide increases until 47 and 78 meV, respectively.

Several factors affect the electronic properties of the graphene (silicene) - (2D-SiC) interface: hybridization of the states of the electron valence band of graphene (silicene) and SiC, charge transfer from graphene (silicene) to silicon carbide, and lattice matching between graphene (silicene) and the SiC surface. The band gap opening of graphene on the 2D-SiC is associated with the hybridization between graphene- and SiC-derived electronic states. In "graphene on one-, two-, three-layer silicon carbide" system, the hybridization occurs between the 2p-electrons of the carbon of the graphene sheet with the 2p-electrons of the carbon of the silicon carbide. In addition, in the "graphene-three-layer 2D-SiC" system, the hybridization also appears between 2s-electrons of carbon with 3p-electrons of silicon. The hybridization is associated with the changes induced through a significant rearrangement of the structure of the upper SiC layer, which directly interacts with graphene. The SiC structure undergoes even stronger changes when silicene is placed on this two-dimensional material. In addition, in this case, the structure of the silicene itself also changes significantly. The emerging intercalation of silicene in SiC causes the hybridization. In the "silicene-one-, two-, and three-layer 2D-SiC" systems, the hybridization occurs between carbide 2p electrons and 3p electrons of the silicene sheet. In this case, the opening band gap in silicene turns out to be noticeably larger than in
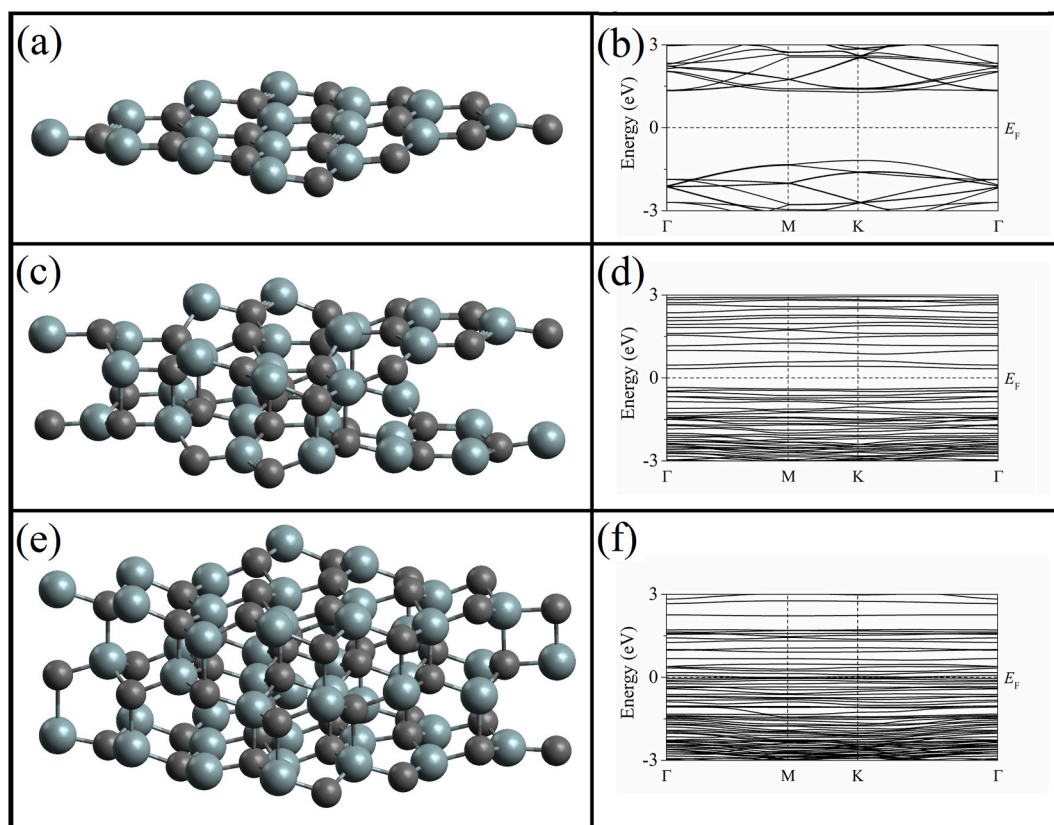
**Fig. 5.** Geometrical structures of (a) one-, (c) two-, and (e) three-layer 2D-SiC obtained on a silicene sheet, which is not illustrated; the band structures in these systems, i. e. in the presence of (b) one-, (d) two- and (f) three layers of SiC are shown without direct contribution from silicene.

graphene. In addition, in silicene on silicon carbide, an increase in the number of 2D-SiC layers to three (Fig. 7c) leads to the disappearance of the Dirac cones. In this case, a transition occurs from a semiconductor with a direct band gap to a semiconductor with an indirect band gap, the width of which is 17 meV. The above transition occurs when the average vertical displacements of Si atoms in silicene exceed the critical value, so that the distance between silicene and 2D-SiC will decrease by more than 1 Å.

There is a quite definite relation between the type of the band structure and the form of the density of electronic states. For example, when the band is very flat in a certain range of energies at finite $k$, then a high density of states is observed, due to the presence of many different values of $k$ (states) corresponding to almost the same energy. The calculated densities of electronic states agree with the determined band structure. The densities of states near the Fermi level takes zero values in a narrow energy range, which indicates the type of conductivity of the obtained hybrid structures, which prevails in semiconductor materials.

## 4. Conclusion

We investigated by the DFT calculations the changes in the structure, energy and electronic properties of hybrid two-dimensional materials formed by combining graphene or silicene with layered silicon carbide, depending on the number of SiC layers. Calculations show that the structural and energy properties of graphene change slightly when combined with two-dimensional silicon carbide. In this case, however, a narrow band gap of ~15–22 meV opens in graphene, which, like the Dirac cone, is present regardless of the SiC thickness. In this case, the interlayer distance in multilayer silicon carbide significantly decreases, and the cohesion energy between its layers increases significantly. A different picture is observed when silicene is combined with layered silicon carbide. Both geometric and energy characteristics of silicene are

strongly dependent on the number of layers present in SiC. In this case, with an increase in the number of SiC layers, silicene expands due to an increase in the distance between its sublattices in the z direction. However, the distortion of its structure in the horizontal plane is minimal. Calculations show that in the formed hybrid structure, graphene or silicene sheets acquire a positive total charge, while silicon carbide is negatively charged. Significant structural rearrangements occur in the silicon carbide itself when a third layer is added. The SiC structure fragmentarily approaches the structure of bulk 4H–SiC. The combination of silicene with silicon carbide affects its electronic structure. In particular, in the presence of one- and two-layer SiC, when the vertical displacements of Si atoms in silicene have not yet reached critical values, its band gap remains straight and expands first to 47 and then to 78 meV. An alternative change in the electronic properties occurs at very strong vertical displacements of Si atoms in silicene. At the same time, the band gap of silicene loses straight form and decreases to 17 meV, and the Dirac cone disappears completely.

Thus, when creating a two-dimensional hybrid material C(Si)-2D-SiC, it should be taken into account that graphene is not very sensitive to the number of layers contained in SiC, while the combination of silicene with three-layer SiC causes significant rearrangements in silicene structure and significant changes in electronic properties.

## Author contributions

Alexander Galashev CRediT roles: Conceptualization; Methodology; Supervision; Investigation; Writing – original draft; Alexey Vorob'ev CRediT roles: Data curation; Investigation; Software; Visualization; Writing – original draft.
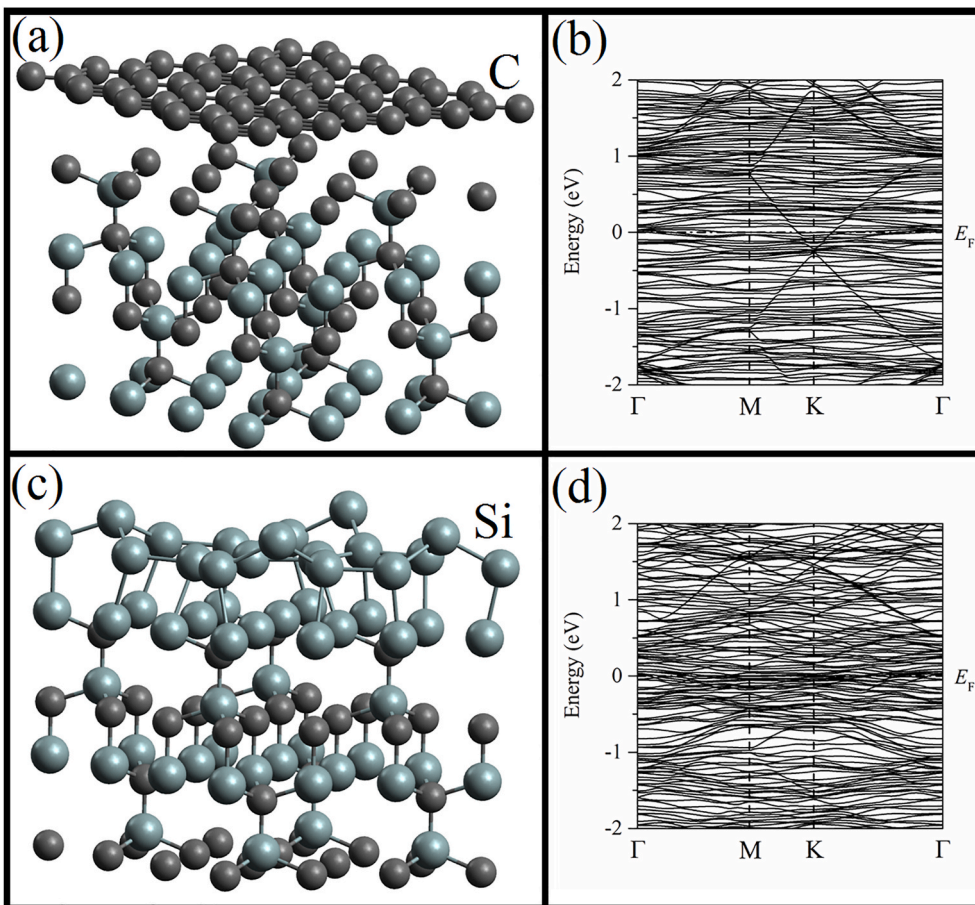
**Fig. 6.** Geometrical structures: (a) graphene and (c) silicene, located on two bilayers of 4H–SiC bulk structure; the band structures of the systems: (b) "graphene on 4H–SiC" and (d) "silicene on 4H–SiC".
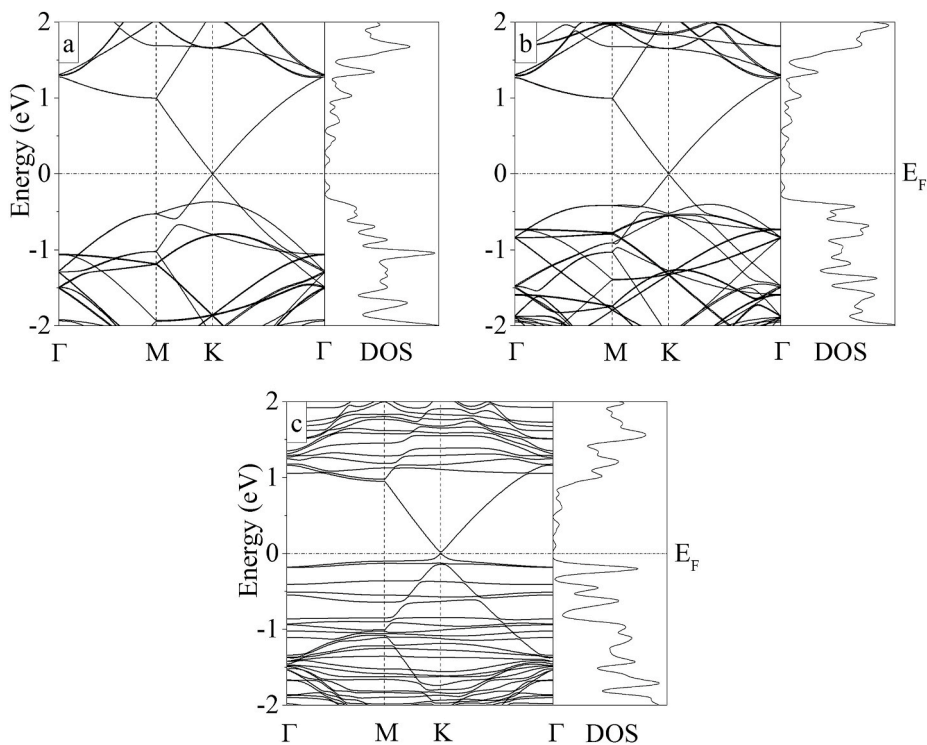


**Fig. 7.** Band structures and spectra of electronic states of the "graphene on silicon carbide" systems with: (a) one-, (b) two- and (c) three-layers in 2D-SiC.
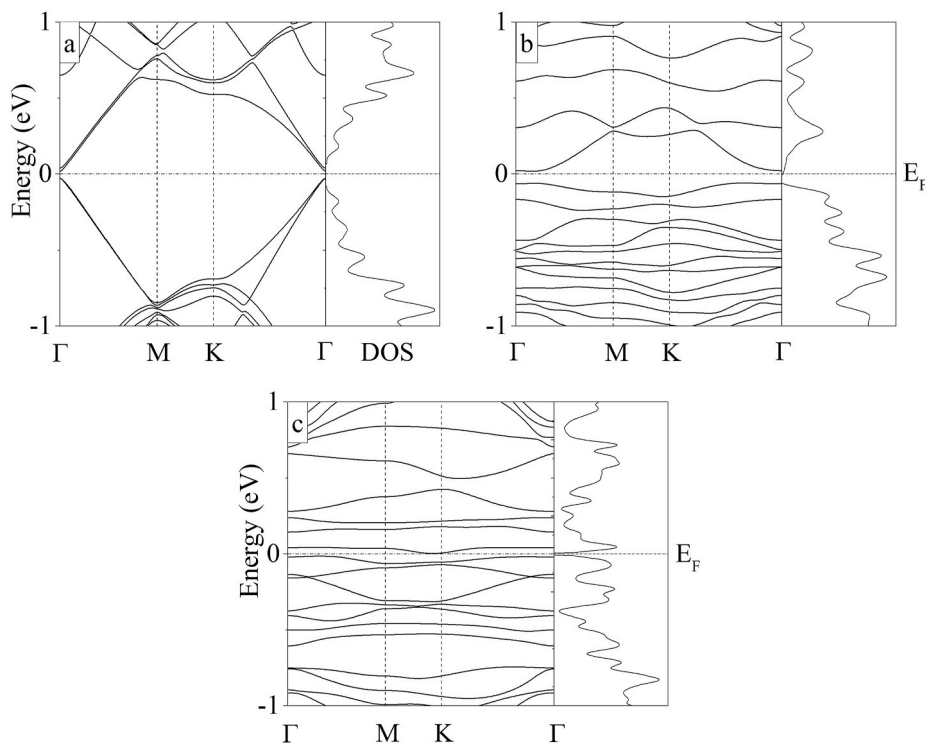
**Fig. 8.** Band structures and spectra of electronic states of the "silicene on silicon carbide" systems with: (a) one-, (b) two- and (c) three layers in 2D-SiC.

## Declaration of competing interest

The authors declare that they have no known competing financial interests or personal relationships that could have appeared to influence the work reported in this paper.

## Acknowledgements

## References

[1] K.S. Novoselov, A.K. Geim, S. V Morozov, D. Jiang, Y. Zhang, S.V. Dubonos, I. V. Grigorieva, A.A. Firsov, Electric field effect in atomically thin carbon films, Science 306 (2004) 666–669, https://doi.org/10.1126/science.1102896.

[2] A.K. Geim, K.S. Novoselov, The rise of graphene, Nat. Mater. 6 (2007) 183–191, https://doi.org/10.1038/nmat1849.

[3] H. Zhang, H. Xu, Nanocrystalline silicon carbide thin film electrodes for lithium-ion batteries, Solid State Ionics 263 (2014) 23–26, https://doi.org/10.1016/j.ssi.2014.04.020.

[4] I. Shtepliuk, V. Khranovskyy, R. Yakimova, Combining graphene with silicon carbide: synthesis and properties – a review, Semicond. Sci. Technol. 31 (2016) 113004, https://doi.org/10.1088/0268-1242/31/11/113004.

[5] R.S. Singh, D. Li, Q. Xiong, I. Santoso, X. Yu, W. Chen, A. Rusydi, A.T.S. Wee, Anomalous photoresponse in the deep-ultraviolet due to resonant excitonic effects in oxygen plasma treated few-layer graphene, Carbon 106 (2016) 330–335, https://doi.org/10.1016/j.carbon.2016.05.026.

[6] A. Balandin, S. Ghosh, W. Bao, I. Calizo, D. Teweldebrhan, F. Miao, C.N. Lau, Superior thermal conductivity of single-layer graphene, Nano Lett. 8 (2008) 902–907, https://doi.org/10.1021/nl0731872.

[7] H. Chen, M.B. Müller, K.J. Gilmore, G.G. Wallace, D. Li, Mechanically strong, electrically conductive, and biocompatible graphene paper, Adv. Mater. 20 (2010) 3557–3561, https://doi.org/10.1002/adma.200800757.

[8] Z. Sun, S. Fang, Y.H. Hu, 3D Graphene materials: from understanding to design and synthesis control, Chem. Rev. 120 (2020) 10336–10453, https://doi.org/10.1021/acs.chemrev.0c00083.

[9] L. Song, L. Ci, H. Lu, P.B. Sorokin, C. Jin, J. Ni, A.G. Kvashnin, D.G. Kvashnin, J. Lou, B.I. Yakobson, P.M. Ajayan, Large scale growth and characterization of atomic hexagonal boron nitride layers, Nano Lett. 10 (2010) 3209–3215, https://doi.org/10.1021/nl1022139.

[10] A.J. Mannix, X.-F. Zhou, B. Kiraly, J.D. Wood, D. Alducin, B.D. Myers, X. Liu, B. L. Fisher, U. Santiago, J.R. Guest, M.J. Yacaman, A. Ponce, A.R. Oganov, M. C. Hersam, N.P. Guisinger, Synthesis of borophenes: anisotropic, two-dimensional boron polymorphs, Science 350 (2015) 1513–1516, https://doi.org/10.1126/science.aad1080.

[11] E. Bianco, S. Butler, S. Jiang, O.D. Restrepo, W. Windl, J.E. Goldberger, Stability and exfoliation of germanane: a germanium graphane analogue, ACS Nano 7 (2013) 4414–4421, https://doi.org/10.1021/nn4009406.

[12] L. Li, Y. Yu, G.J. Ye, Q. Ge, X. Ou, H. Wu, D. Feng, X.H. Chen, Y. Zhang, Black phosphorus fieldeffect transistors, Nat. Nanotechnol. 9 (2014) 372–377, https://doi.org/10.1038/nnano.2014.35.

[13] P. Vogt, P. De Padova, C. Quaresima, J. Avila, E. Frantzeskakis, M.C. Asensio, A. Resta, B. Ealet, G. Le Lay, Silicene: compelling experimental evidence for graphenelike two-dimensional silicon, Phys. Rev. Lett. 108 (2012) 155501, https://doi.org/10.1103/PhysRevLett.108.155501.

[14] L. Meng, Y. Wang, L. Zhang, S. Du, R. Wu, L. Li, Y. Zhang, Buckled silicene formation on Ir(111), Nano Lett. 13 (2013) 685–690, https://doi.org/10.1021/nl304347w.

[15] E. Scalise, K. Iordanidou, V.V. Afanas, A. Stesmans, M. Houssa, Silicene on non-metallic substrates: recent theoretical and experimental advances, Nano Res. 11 (2018) 1169–1182, https://doi.org/10.1007/s12274-017-1777-y.

[16] A. Fleurence, R. Friedlein, T. Ozaki, H. Kawai, Y. Wang, Y. Yamada-Takamura, Experimental evidence for epitaxial silicene on diboride thin films, Phys. Rev. Lett. 108 (2012) 245501, https://doi.org/10.1103/PhysRevLett.108.245501.

[17] T. Aizawa, S. Suehara, S. Otani, Silicene on zirconium carbide (111), J. Phys. Chem. C 118 (2014) 23049–23057, https://doi.org/10.1021/jp505602c.

[18] M. De Crescenzi, I. Berbezier, M. Scarselli, P. Castrucci, M. Abbarchi, A. Ronda, F. Jardali, J. Park, H. Vach, D. Fisica, R. Tor, Formation of silicene nanosheets on graphite, ACS Nano 10 (2016) 11163–11171, https://doi.org/10.1021/acsnano.6b06198.

[19] L. Huang, Y. Zhang, Y. Zhang, W. Xu, Y. Que, E. Li, J. Pan, Y. Wang, Y. Liu, S. Du, S. T. Pantelides, H. Gao, Sequence of silicon monolayer structures grown on a Ru surface: from a herringbone structure to silicene, Nano Lett. 17 (2017) 116–1166, https://doi.org/10.1021/acs.nanolett.6b04804.

[20] A.Y. Galashev, K.A. Ivanichkina, Computational investigation of a promising Si–Cu anode material, Phys. Chem. Chem. Phys. 21 (2019) 12310–12320, https://doi.org/10.1039/C9CP01571J.

[21] A.Y. Galashev, K.A. Ivanichkina, A.S. Vorob'ev, O.R. Rakhmanova, K.P. Katin, M. M. Maslov, Improved lithium-ion batteries and their communication with hydrogen power, Int. J. Hydrogen Energy 46 (2021) 17019–17036, https://doi.org/10.1016/j.ijhydene.2020.11.225.

[22] A.E. Galashev, K.A. Ivanichkina, A.S. Vorob'ev, O.R. Rakhmanova, Structure and stability of defective silicene on Ag(001) and Ag(111) substrates: a computer experiment, Phys. Solid State 59 (2017) 1242–1252, https://doi.org/10.1134/S1063783417060087.

[23] A.Y. Galashev, A.S. Vorob'ev, DFT study of silicene on metal (Al, Ag, Au) substrates of various thicknesses, Phys. Lett. 408 (2021) 127487, https://doi.org/10.1016/j.physleta.2021.127487.

[24] A.Y. Galashev, K.A. Ivanichkina, Computer test of a new silicone anode for lithium-ion batteries, ChemElectroChem 6 (2019) 1525–1535, https://doi.org/10.1002/celc.201900119.

[25] A.Y. Galashev, K.A. Ivanichkina, Silicene anodes for lithium-ion batteries on metal substrates, J. Electrochem. Soc. 167 (2020), 050510, https://doi.org/10.1149/1945-7111/ab717a.

[26] A.E. Galashev, O.R. Rakhmanova, K.A. Ivanichkina, Graphene and graphite supports for silicene stabilization: a computation study, J. Struct. Chem. 59 (2018) 877–883, https://doi.org/10.1134/S0022476618040194.

[27] A.Y. Galashev, K.A. Ivanichkina, K.P. Katin, M.M. Maslov, Computer test of a modified silicene/graphite anode for lithium-ion batteries, ACS Omega 5 (2020) 13207–13218, https://doi.org/10.1021/acsomega.0c01240.

[28] A.Y. Galashev, A.S. Vorob'ev, Electronic and mechanical properties of silicene after nuclear transmutation doping with phosphorus, J. Mater. Sci. 55 (2020) 11367–11381, https://doi.org/10.1007/s10853-020-04860-8.

[29] H. Lin, W. Qiu, J. Liu, L. Yu, S. Gao, H. Yao, Y. Chen, Silicene: wet-chemical exfoliation synthesis and biodegradable tumor nanomedicine, Adv. Mater. 31 (2019) 1903013, https://doi.org/10.1002/adma.201903013.

[30] H. Li, H.-X. Fu, S. Meng, Silicene: from monolayer to multilayer – a concise review Chin, Phys. Biol. 24 (2015), 086102, https://doi.org/10.1088/1674-1056/24/8/086102.

[31] G.L. Lay, Silicene transistors, Nat. Nanotechnol. 10 (2015) 202–203, https://doi.org/10.1038/nnano.2015.10.

[32] W. Hu, N. Xia, X. Wu, Z. Li, J. Yang, Silicene as a highly sensitive molecule sensor for $NH_3$, NO and $NO_2$, Phys. Chem. Chem. Phys. 16 (2014) 6957–6962, https://doi.org/10.1039/c3cp55250k.

[33] K. Zberecki, M. Wierzbicki, J. Barnas, R. Swirkowicz, Thermoelectric effects in silicene nanoribbons, Phys. Rev. B 88 (2013) 115404, https://doi.org/10.1103/PhysRevB.88.115404.

[34] R. Cheung, Introduction to Silicon Carbide Microelectromechanical Systems (MEMS), Imperial College Press, London, 2012.

[35] A. Mattausch, O. Pankratov, *Ab initio* study of graphene on SiC, Phys. Rev. Lett. 99 (2007), 076802, https://doi.org/10.1103/PhysRevLett.99.076802.

[36] H. Şahin, S. Cahangirov, M. Topsakal, E. Bekaroglu, E. Akturk, R.T. Senger, S. Ciraci, Monolayer honeycomb structures of group-IV elements and III-V binary compounds: first-principles calculations, Phys. Rev. B 80 (2009) 155453, https://doi.org/10.1103/PhysRevB.80.155453.

[37] H.C. Hsueh, G.Y. Guo, S.G. Louie, Excitonic effects in the optical properties of a SiC sheet and nanotubes, Phys. Rev. B 84 (2011), 085404, https://doi.org/10.1103/PhysRevB.84.085404.

[38] X. Lin, S. Lin, Y. Xu, A.A. Hakro, T. Hasan, B. Zhang, B. Yu, J. Luo, E. Li, H. Chen, Ab initio study of electronic and optical behavior of two-dimensional silicon carbide, J. Mater. Chem. C 1 (2013) 2131–2135, https://doi.org/10.1039/C3TC00629H.

[39] S. Lin, S. Zhang, X. Li, W. Xu, X. Pi, X. Liu, F. Wang, H. Wu, H. Chen, Quasi-two-dimensional SiC and $SiC_2$: interaction of silicon and carbon at atomic thin lattice plane, J. Phys. Chem. C 119 (2015), https://doi.org/10.1021/acs.jpcc.5b04113, 19772–19779.

[40] S. Chabi, H. Chang, Y. Xia, Y. Zhu, From graphene to silicon carbide: ultrathin silicon carbide flakes, Nanotechnology 27 (2016), 075602, https://doi.org/10.1088/0957-4484/27/7/075602.

[41] T. Susi, V. Skakalova, A. Mittelberger, P. Kotrusz, M. Hulman, T.J. Pennycook, C. Mangler, J. Kotakoski, J.C. Meyer, Computational insights and the observation of SiC nanograin assembly: towards 2D silicon carbide, Sci. Rep. 7 (2017) 4399, https://doi.org/10.1038/s41598-017-04683-9.

[42] R.S. Singh, A. Solanki, Modulation of electronic properties of silicon carbide nanotubes via sulphur-doping: an ab initio study, Phys. Lett. 380 (2016) 1201–1204, https://doi.org/10.1016/j.physleta.2016.01.029.

[43] R.S. Singh, Hydrogen adsorption on sulphur-doped SiC nanotubes, Mater. Res. Express 3 (2016), 075014, https://doi.org/10.1088/2053-1591/3/7/075014.

[44] B.P. Singh, B.K. Jena, S. Bhattacharjee, L. Besra, Development of oxidation and corrosion resistance hydrophobic graphene oxide-polymer composite coating on copper, Surf. Coating. Technol. 232 (2013) 475–481, https://doi.org/10.1016/j.surfcoat.2013.06.004.

[45] A.Y. Galashev, O.R. Rakhmanova, Promising two-dimensional nanocomposite for the anode of the lithium-ion batteries. Computer simulation, Physica E Low Dimens. Syst. Nanostruct. 126 (2021) 114446, https://doi.org/10.1016/j.physe.2020.114446.

[46] Z.Y. Al Balushi, K. Wang, R.K. Ghosh, R.A. Vila, S.M. Eichfeld, J.D. Caldwell, X. Qin, Y.-C. Lin, P.A. DeSario, G. Stone, S. Subramanian, D.F. Paul, R.M. Wallace, S. Datta, J.M. Redwing, J.A. Robinson, Two-dimensional gallium nitride realized via graphene encapsulation, Nat. Mater. 15 (2016) 1166–1171, https://doi.org/10.1038/nmat4742.

[47] B. Pecz, G. Nicotra, F. Giannazzo, R. Yakimova, A. Koos, A. Kakanakova-Georgieva, Indium nitride at the 2D limit, Adv. Mater. 33 (2021) 2006660, https://doi.org/10.1002/adma.202006660.

[48] A. Kakanakova-Georgieva, G.K. Gueorguiev, D.G. Sangiovanni, N. Suwannaharn, I.G. Ivanov, I. Cora, B. Pecz, G. Nicotra, F. Giannazzo, Nanoscale phenomena ruling deposition and intercalation of AlN at the graphene/SiC interface, Nanoscale 12 (2020) 19470, https://doi.org/10.1039/D0NR04464D.

[49] F. Giannazzo, G. Greco, F. Roccaforte, S.S. Sonde, Vertical transistors based on 2D materials: status and prospects, Crystals 8 (2018) 70, https://doi.org/10.3390/cryst8020070.

[50] A.K. Geim, I.V. Grigorieva, Van der Waals heterostructures, Nature 499 (2013) 419–425, https://doi.org/10.1038/nature12385.

[51] D. Jariwala, T.J. Marks, M.C. Hersam, Mixed-dimensional van der Waals heterostructures, Nat. Mater. 16 (2017) 170–181, https://doi.org/10.1038/nmat4703.

[52] L. Britnell, R.V. Gorbachev, R. Jalil, B.D. Belle, F. Schedin, A. Mishchenko, T. Georgiou, M.I. Katsnelson, L. Eaves, S.V. Morozov, N.M.R. Peres, J. Leist, A.K. Geim, K.S. Novoselov, L.A. Ponomarenko, Field-effect tunneling transistor based on vertical graphene heterostructures, Science 335 (2012) 947–950, https://doi.org/10.1126/science.1218461.

[53] D. Sarkar, X. Xie, W. Liu, W. Cao, J. Kang, Y. Gong, S. Kraemer, P.M. Ajayan, K. Banerjee, A subthermionic tunnel field-effect transistor with an atomically thin channel, Nature 526 (2015) 91–95, https://doi.org/10.1038/nature15387.

[54] H. Yang, J. Heo, S. Park, H.J. Song, D.H. Seo, K.-E. Byun, P. Kim, I. Yoo, H.-J. Chung, K. Kim, Graphene barristor, a triode device with a gate-controlled Schottky barrier, Science 336 (2012) 1140–1143, https://doi.org/10.1126/science.1220527.

[55] J.M. Soler, E. Artacho, J.D. Gale, A. Garcia, J. Junquera, P. Ordejon, D. Sanchez-Portal, The SIESTA method for ab initio order-N materials simulation, J. Phys. Condens. Matter 14 (2002) 2745, https://doi.org/10.1088/0953-8984/14/11/302.

[56] J.E. Padilha, R.B. Pontes, Free-Standing Bilayer Silicene: the effect of stacking order on the structural, electronic, and transport properties, J. Phys. Chem. C 119 (2015) 3818–3825, https://doi.org/10.1021/jp512489m.

[57] M. Dion, H. Rydberg, E. Schroder, D.C. Langreth, B.I. Lundqvist, Van der Waals density functional for general geometries, Phys. Rev. Lett. 92 (2004) 246401, https://doi.org/10.1103/PhysRevLett.92.246401.

[58] T. Wang, C. Li, C. Xia, L. Yin, Y. An, S. Wei, X. Dai, Silicene/BN vdW heterostructure as an ultrafast ion diffusion anode material for Na-ion battery, Physica E 122 (2020) 114146, https://doi.org/10.1016/j.physe.2020.114146.

[59] H.J. Monkhorst, J.D. Pack, Special points for Brillouin-zone integrations, Phys. Rev. B 13 (1976) 5188, https://doi.org/10.1103/PhysRevB.13.5188.

[60] C.F. Guerra, J.W. Handgraaf, E.J. Baerends, F.M. Bickelhaupt, Voronoi deformation density (VDD) charges: assessment of the Mulliken, Bader, Hirshfeld, Weinhold, and VDD methods for charge analysis, J. Comput. Chem. 25 (2) (2003) 189–210, https://doi.org/10.1002/jcc.10351.

[61] N.D. Drummond, V. Zólyomi, V.I. Fal'ko, Electrically tunable band gap in silicene, Phys. Rev. B 85 (2012), 075423, https://doi.org/10.1103/PhysRevB.85.075423.

[62] B.D. Oli, C. Bhattarai, B. Nepal, N.P. Adhikari, First-principles study of adsorption of alkali metals (Li, Na, K) on graphene, Adv. Nanomat. and Nanotech. 143 (2013) 515–529, https://doi.org/10.1007/978-3-642-34216-5_51.

[63] X.H. Liu, J.W. Suk, N.G. Boddeti, L. Cantley, L.D. Wang, J.M. Gray, et al., Large arrays and properties of 3-terminal graphene nanoelectromechanical switches, Adv. Mater. 26 (2014) 1571–1576, https://doi.org/10.1002/adma.201304949.

[64] J.W. Suk, K. Kirk, Y.F. Hao, N.A. Hall, R.S. Ruoff, Thermoacoustic sound generation from monolayer graphene for transparent and flexible sound sources, Adv. Mater. 24 (2012) 6342–6347, https://doi.org/10.1002/adma.201201782.

[65] S.S. Chen, L. Brown, M. Levendorf, W.W. Cai, S.Y. Ju, J. Edgeworth, et al., Oxidation resistance of graphene-coated Cu and Cu/Ni alloy, ACS Nano 5 (2011) 1321–1327, https://doi.org/10.1021/nn103028d.

[66] S.R. Na, J.W. Suk, R.S. Ruoff, R. Huang, K.M. Liechti, Ultra long-range interactions between large area graphene and silicon, ACS Nano 8 (2014) 11234–11242, https://doi.org/10.1021/nn503624f.

[67] S.P. Koenig, N.G. Boddeti, M.L. Dunn, J.S. Bunch, Ultrastrong adhesion of graphene membranes, Nat. Nanotechnol. 6 (2011) 543–546, https://doi.org/10.1038/nnano.2011.123.

[68] I. Shtepliuk, T. Iakimov, V. Khranovskyy, J. Eriksson, F. Giannazzo, R. Yakimova, Role of the potential barrier in the electrical performance of the graphene/SiC interface, Crystals 7 (6) (2017) 162, https://doi.org/10.3390/cryst7060162.

[69] S. Sonde, F. Giannazzo, V. Raineri, R. Yakimova, J.-R. Huntzinger, A. Tiberj, J. Camassel, Electrical properties of the graphene/4 H -SiC (0001) interface probed by scanning current spectroscopy, Phys. Rev. B 80 (2009) 241406, https://doi.org/10.1103/PhysRevB.80.241406 (R).

[70] M. Inaba, K. Suzuki, M. Shibuya, C.-Y. Lee, Y. Masuda, N. Tomatsu, W. Norimatsu, A. Hiraiwa, M. Kusunoki, H. Kawarada, Very low Schottky barrier height at carbon nanotube and silicon carbide interface, Appl. Phys. Lett. **106** (2015) 123501, https://doi.org/10.1063/1.4916248.

[71] X. Tang, J. Katcki, E. Dubois, V. Bayot, Very low Schottky barrier to n-type silicon with PtEr-stack silicide, Solid State Electron. 47 (2003) 2105–2111, https://doi.org/10.1016/S0038-1101(03)00256-9.